

**NASA Technical Memorandum 104123**

**A RELATIVE-INTENSITY TWO-COLOR PHOSPHOR  
THERMOGRAPHY SYSTEM**

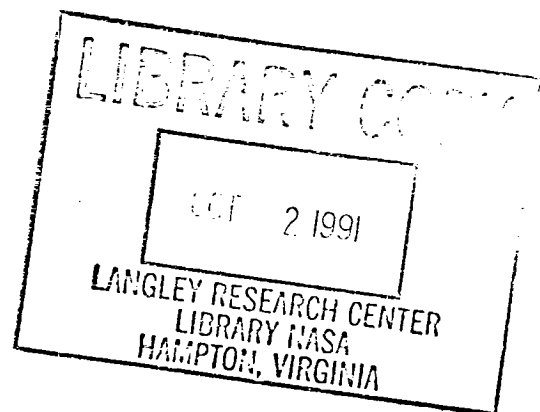
**N. Ronald Merski**

**September 1991**



National Aeronautics and  
Space Administration

Langley Research Center  
Hampton, Virginia 23665-5225



**FOR REFERENCE**

NOT TO BE TAKEN FROM THIS ROOM



## Abstract

The NASA Langley Research Center has developed a relative-intensity two-color phosphor thermography system. This system has become a standard technique for acquiring aerothermodynamic data in Langley's Hypersonic Facilities Complex (HFC). The relative intensity theory and its application to the Langley phosphor thermography system is discussed along with the investment casting technique which is critical to the utilization of the phosphor method for aerothermodynamic studies. Various approaches to obtaining quantitative heat transfer data using thermographic phosphors are addressed and comparisons between thin-film data and thermographic phosphor data on an orbiter-like configuration are presented. In general, data from these two techniques are in good agreement. A discussion is given on the application of phosphors to integration heat transfer data reduction techniques (i.e. the thin-film method) and preliminary heat transfer data obtained on a calibration sphere using thin-film equations are presented. Finally, plans for a new phosphor system which uses target recognition software are discussed.



## Introduction

A renewed interest occurred in hypersonics in this country in the mid 1980's. Several new vehicle concepts came to the fore such as the National Aero-Space Plane (NASP), the Assured Crew Return Vehicle (ACRV), the Personnel Launch System (PLS), the Advanced Manned Launch System (AMLS), The Aeroassisted Space Transfer Vehicles (ASTV), and the Aeroassist Flight Experiment (AFE). These programs and others have challenged aerodynamicists and aerothermodynamicists to determine the aerodynamic characteristics and thermal loads for proposed vehicles in a timely manner, thereby requiring fast-paced techniques to provide detailed heat transfer distributions. This activity revealed the need for an aerothermodynamic measurement technique capable of providing large amounts of reliable data in a quick and efficient manner.

Relatively recent improvements made in video acquisition technology are beginning to have a profound influence on aerothermodynamic data acquisition. Techniques which use video acquisition such as phosphor thermography or infrared thermography have demonstrated the capability to provide qualitative information via thermal mappings and are now on the verge of producing respectable quantitative heat transfer data -- thus challenging standard techniques such as thin-film resistance gages, coaxial thermocouples and thin-skin transient calorimeter gages. Indeed, optical systems which use video can go one step further than traditional instrumentation in that they can obtain global heating characteristics while the latter provide heating at discrete points. This capability saves a large amount of time in the model fabrication process since it does not require installation and calibration of a large number of discrete gages and it also provides more detailed surface distributions for calibration of computational fluid dynamic (CFD) and engineering computer codes.

To address the aerothermodynamic measurement challenges of the nineties, Langley has been making use of video acquisition technology in the form of a relative intensity two-color phosphor thermography system. A large amount of the early development of this system was performed by G.M. Buck<sup>1,2,3</sup> and this technique is now coming to fruition. In the last year or so, phosphor thermography has become a standard method for acquiring aerothermodynamic data in Langley's Hypersonic Facilities Complex (HFC).<sup>4</sup> The system has been used successfully on a number of projects which include the HL20 and HL20A lifting body concepts (Langley proposed candidates for ACRV and PLS), a code calibration experiment for an orbiter-like configuration, the National Aerospace Plane (NASP) and a proposed ballute configuration to control the AFE Solid Rocket Motor (SRM) trajectory during entry into the atmosphere.

The purpose of this paper is to review various aspects of the two-color phosphor technique including relative-intensity two-color phosphor thermography theory, model fabrication, wind tunnel facilities and quantitative heat transfer data reduction techniques. In addition, the results of some comparisons with the thin-film technique and with computational fluid dynamics will be presented and the future of the thermographic phosphor method at Langley will be discussed.

### Symbols

a,b	logarithmic intensity function coefficients
A,B	curve-fit coefficients
c	heat capacity
d,e,f	distances from lens plane to selected model focus point
F	logarithmic intensity function
h	heat transfer coefficient, $\dot{q} / (T_{aw} - T_s)$
I	intensity
k	thermal conductivity
L	length
$\dot{q}$	heat transfer rate
s	Laplace transform variable
t	time
T	temperature
x	distance normal to surface
y	lateral distance normal to model centerline
$\alpha$	thermal diffusivity, $k/\rho c$
$\beta$	thermal product $(\rho c k)^{1/2}$
$\theta$	$T - T_i$
$\lambda$	$h(t)^{1/2}/\beta$

$\rho$  density  
 $\tau$  time integration dummy variable

Subscripts:

aw adiabatic wall  
G green signal  
i initial  
ph phosphors  
R red signal  
s surface

A bar over a variable denotes Laplace transform

Background

Thermographic phosphors are materials that emit or fluoresce visible light when they are illuminated with ultraviolet (UV) light. Their emission intensity is dependent on their temperature. Typically, electrons within a phosphor populate either the valence energy band or the conduction energy band as shown in Fig. 1<sup>5</sup>. However, with the addition of an impurity into the crystalline lattice of the phosphor, other possible intermediate energy levels are possible. When the phosphors are exposed to ultraviolet radiation, electrons are raised from the valence energy band to the conduction band. Fluorescence occurs when electrons emit photons upon relaxation to the lower intermediate energy states. However, if the intermediate energy level is close enough to the valence level, electrons from the valence band can be thermally excited and raised to the intermediate energy level. When this occurs, electrons returning from the conduction band must compete with the thermally excited electrons from the valence band. As the temperature increases, less electrons are able to go from the conduction band to the intermediate band and the emission intensity decreases. Eventually, if the temperature of the phosphor rises enough, no relaxation of the electrons in the conduction band can occur; consequently there is no fluorescence and the phosphor is effectively quenched.

Because of their temperature dependence, phosphors have an application in surface heat transfer studies in hypersonic wind tunnels. A heat transfer model can be fabricated, coated with a

phosphor, mounted in a wind tunnel, illuminated with ultraviolet light and viewed with a camera. By examining the intensity of phosphor emission, the temperature can theoretically be determined over the entire surface of the model. However, use of a coating which fluoresces at a single wavelength of light can be impractical, especially if quantitative data is desired. While the intensity of the surface fluorescence at a point on the model changes due to temperature, it is also dependent on the amount of incident light at the location. Since a model with a complicated geometry cannot easily be uniformly illuminated, corrections are required to account for uneven lighting. In addition, it is very difficult to calibrate an absolute intensity system.

In order to circumvent the problems associated with a single band-width type system, a relative intensity two-color method can be used. With this technique, a phosphor mixture is used which emits two different colors of light. The ratio of the emission intensities of the two colors can be shown to be independent of the amount of irradiance of ultraviolet light.<sup>3</sup> Hence, concerns about non-uniform illumination of the model associated with a single color phosphor system are eliminated with the two-color method since the ratio of intensities is only dependent on temperature and not any sort of local curvature effects.

A further advantage of the two-color thermography technique is that the surface fluorescence of each color can actually be measured as a relative intensity value which is some logarithmic function of the absolute intensity for each color. For two colors, this can be shown mathematically as:

$$F_R = a \cdot \log(I_R) + b_R \quad (1)$$

$$F_G = a \cdot \log(I_G) + b_G \quad (2)$$

Subtracting Equation 2 from Equation 1 yields:

$$F_{RG} = F_R - F_G = a \cdot \log(I_R/I_G) + b_{RG} \quad (3)$$

Since the ratio of intensities is temperature dependent, the difference between the relative intensity values,  $F_{RG}$ , is also a function of temperature. This relative intensity approach makes calibration of a phosphor thermography system much easier than an absolute intensity calibration procedure.



## Description of Present Relative-Intensity Two-Color Phosphor Thermography System

As previously stated, most of the development of the relative intensity two-color phosphor thermography method used at Langley was performed by G. M. Buck.<sup>1,2,3</sup> This method has been shown to yield accurate quantitative temperature distributions on wind tunnel models. Basically, a model is first sprayed with a mixture consisting of two phosphors and a colloidal silica binder. One phosphor, Radelin\* No. 1807, is a zinc cadmium sulfide with trace impurities of silver and nickel and it fluoresces in the green portion of the visible spectrum. The other, a rare-Earth phosphor made up of lanthanum oxysulfide with one percent europium, fluoresces in the red region of the spectrum. Once a model is prepared and mounted in a wind tunnel, it is irradiated with long wavelength ultraviolet light from five, 100 watt mercury arc lamps with band-pass filters at 365 nm as shown in Fig. 2. The resulting phosphor emission from the model is viewed with a 3 CCD (Charge Coupled Device) color camera driven by a 386-based personal computer (PC) through an image processor. Framing rate of the camera can be controlled through the image processor at a maximum acquisition frequency of up to 30 Hertz. Once the camera obtains an image, internal filters in the camera then separate the RGB signal into constituent red, green and blue signals. Next, the red and green signals are digitized in the image processor to a resolution of 512 x 512 pixels. The digitized images are saved for later heat transfer data reduction and at the same time are immediately converted on-line to temperature values in the form of color contouring on the model which can be viewed on a high resolution color monitor or printed out on a color printer.

### Model Fabrication

Several points should be considered in the fabrication of models for use with thermographic phosphors. First, since the models are used to infer heat transfer distributions, they must be made of materials which are good insulators and are homogenous. In addition, the fabrication process must allow for complicated shapes (e.g. models with thin control surfaces) and, if possible, it should be quick and cost effective. A great deal of research has gone into developing such a procedure for fabricating thermographic phosphor models and an investment casting technique has been developed by Buck and Vasquez.<sup>6</sup>

The first step in this casting technique is to obtain a mold. Generally a pattern is cut on a computer milling machine using the aerolines of the vehicle. This pattern can be made out of wax, aluminum, foam or wood. Once the pattern is made, it is used to

---

\*Tradename of the USR Optonix Corp.

make either a wax-injection mold or a slush mold. The wax-injection mold is made by pouring an epoxy around the pattern or by coating the model with a hard polyester. One problem with making a mold in this way is that there can be a small amount of shrinkage associated with the pouring and lay-up procedures; however, this approach is good for making complicated shapes. If a high degree of model fidelity is important and if a simple geometry is to be cast, a slush mold can be made. Basically with this type of mold, RTV rubber is poured around the pattern and the pattern is then pulled out of the mold. This method has minimal shrinkage associated with it.

Recently, an alternate method has been used to make wax-injection molds which eliminates the need for a pattern. Basically, the pieces of a mold are made using the computer milling machine. This technique can be time consuming because smaller tools have to be utilized to mill cavities in the mold. Also a high level of ingenuity is required for programming tool paths, especially in the vicinity of sharp edges. A mold made in this manner, however, has no shrinkage associated with it and if the tool paths are properly chosen, it takes less time than the molds made with patterns. This method for fabricating a mold was successfully used to make a ceramic model of the Pegasus Air-Launched Booster. For a 10-inch long model, fabrication tolerances of .004 of an inch or less can be obtained.

Once the molds have been made, they are used to fabricate wax patterns for investment molds. To make a pattern with an injection mold, molten pattern wax is shot into the mold at high pressures which help to reduce wax shrinkage during cooling. After the wax pattern has been shot the mold is separated at the parting lines and the new wax pattern is removed. With the slush mold on the other hand, wax is poured into the mold and then poured back out. This is repeated until a shell has built up which is about one sixteenth of an inch thick.

After the wax patterns have been completed, investment molds are made. The wax patterns are coated with four layers of a hydraulically setting high temperature plaster. The coated pattern is then put in an oven and heated for four hours, during which time the wax melts out and the investment casting shell is made. While the shell is still hot, it is placed in a fluidized fused silica bed, nose forward. After the mold cools, a ceramic slip (usually composed of fused silica) is poured into the mold. When a shell three-sixteenths to a quarter of an inch has formed the excess slip is poured out. An hour later, the investment mold can be peeled off of the ceramic shell and then twenty-four hours after that the shell is dried in an oven. At this point, the "green" shell can be machined if it is necessary and it is then sintered in a kiln at 2150 degrees Fahrenheit for four hours. The model sting is placed

in the shell and the shell is back-filled with a hydraulically setting ceramic. Finally the model is sprayed with a mixture consisting of two types of thermographic phosphors and a colloidal binder.

One problem which can occur during the casting process is the appearance of dark residue lines on thin sections of models (e.g. wings and fins). Unfortunately, the phosphor mixture does not adhere in regions where these dark lines exist. These lines however have been determined to be concentrations of magnesium from the back-fill which is absorbed into the outer shell of the model. By rubbing the affected area with bleach, the lines are easily removed. The presence of the lines however suggests that magnesium might be absorbed in the rest of the model but to a lesser degree. In order to remove any other possible magnesium, the model can be completely dipped in bleach and baked in an oven.

Another problem which occurs during model fabrication is that the phosphor coating dries with a slight roughness. This roughness causes scatter in the thermographic phosphor data and may even change the character of the flow (i.e. induce boundary layer transition to turbulence). Several approaches to circumvent this problem have been attempted. Different binders and even soap have been added to the phosphor coating mixture with poor results thus far. One idea which has shown some promise is to simply add the phosphors to the ceramic slip. Unfortunately, when the model is sintered, the phosphors burn out. So to deal with this situation, hydraulically setting ceramics are being investigated which have lower curing temperatures. Presently, this method needs more refinement because the ceramics which have been used to date are weakened too much by the addition of the phosphors to cast complex geometries.

Although some problems remain to be solved in the making of ceramic thermographic phosphor models, the present techniques represent a significant advance in wind tunnel aerothermodynamic model fabrication. Given the model geometry, a thermographic phosphor model can be fabricated within a month or two. By comparison, a well instrumented thin-film model (i.e. 100 gages) may take from one to three years to design, fabricate, instrument and calibrate, and it does not yield global heating data to the degree obtainable with a thermographic phosphor model.

### Facilities

The two-color phosphor system is used in the Langley Hypersonic Facilities Complex (HFC). The complex, as shown in Table 1, consists of nine hypersonic wind tunnels used for aerodynamic, aerothermodynamic and fluid dynamic studies of hypersonic models. It can provide a Mach number range of 6 to 22, Reynolds numbers of .03 to 40 million per foot, and specific heat

ratios of 1.10 to 1.67<sup>4</sup>. These parameters are achieved using four different test gases (air, CF<sub>4</sub>, nitrogen, and helium).

Most of the development for the two-color phosphor system has been performed in the 31-Inch Mach 10 Tunnel of the HFC. This blowdown facility runs with a total temperature of approximately 1800 °R, and its total pressure can be varied between 350 to 1450 psi to obtain free-stream unit Reynolds numbers between 0.5 and 2x10<sup>6</sup>/foot. It consists of a high pressure air storage system, an electrical resistance heater, settling chamber, nozzle, test section, adjustable second minimum, aftercooler, vacuum pumps and vacuum spheres. It has a contoured, three-dimensional square nozzle which produces a high quality core flow in the test section, ideal for heat transfer and CFD code calibration studies. Models are mounted to an injection system which is housed in a chamber located on the side wall of the test-section as shown in Fig. 3. The hydraulic injection system is isolated from the test section by a sliding door and can inject models into the flow in less than a second. A large optical window is located on the other side of the test section. This window can be used to irradiate phosphor models with ultraviolet radiation and to view models with a camera system. In the near future, an optical mirror will be installed on the injection plate which will allow the phosphor system to obtain simultaneous views of both sides of a test model.

Use of the phosphor system in other facilities is planned for the future. The system will be used in the 15-Inch Mach 6 Tunnel when it is reactivated in July 1991 after having undergone extensive improvements. The Mach 6 tunnel will feature an axisymmetric nozzle which was designed using advanced CFD techniques. Preliminary calibrations of this nozzle have revealed a very high quality, uniform flow with no centerline focusing disturbances. The Mach 6 tunnel will have a hydraulic injection system from the bottom of the test chamber and there will be three large windows for optical viewing. In addition to the 15-Inch Mach 6 Tunnel, the phosphor system will be tested in the 20-Inch Mach 6 CF<sub>4</sub> Tunnel which is scheduled for reactivation in late July 1991. This tunnel has been fitted with a new axisymmetric nozzle and test chamber and like the Mach 6 tunnel, it too has a hydraulic injection system from the bottom of the test chamber and three windows for optical access. Application of the phosphors to this tunnel is particularly interesting because the test gas absorbs infrared radiation and thus does not allow thermal mapping using infrared thermography techniques. Two other tunnels presently being upgraded are planned for use with the phosphor system towards the end of calendar year 1991. They are the 22-Inch Mach 20 Helium and the 20-Inch Mach 17 Nitrogen Tunnels.

### Discussion and Application of Data Reduction Techniques

Presently, three methods are used at LaRC to determine heat transfer coefficients from phosphor thermography data. These methods include a step injection technique like that used for phase-change paint data reduction, a curve-fitting procedure, and an integration method similar to that utilized in the reduction of thin-film data. Each of these three methods will be described in the following sections.

All of the phosphor thermography data reduction techniques used to date assume one dimensional heat conduction normal to the wind tunnel model surface. Thus the governing equation for all three methods is given by:

$$\frac{\partial \theta}{\partial t} = \alpha \frac{\partial^2 \theta}{\partial x^2} \quad (4)$$

In order to solve equation (4), two boundary conditions and one initial condition are needed. Using Fourier's Law, the boundary condition at the surface is given by:

$$-k \frac{\partial \theta}{\partial x} \Big|_{x=0} = \dot{q}_s \quad (5)$$

In addition, using an infinite slab assumption, the boundary condition at  $x=\infty$  is

$$\theta(\infty, t) = 0 \quad (6)$$

For an initial condition, the temperature is assumed to be constant at every location on the model before the injection begins. Thus

$$\theta(x, 0) = 0 \quad (7)$$

Assuming that the phosphor layer on the model does not insulate the model (i.e. has negligible heat capacity and thus is essentially

"invisible") and that the substrate thermal properties are constant, the Laplace transforms of equations (4) through (7) can be combined to yield<sup>5</sup>

$$\bar{\theta}_s = \frac{\bar{q}_s}{\beta\sqrt{s}} \quad (8)$$

Equation (8) is the basis for all three data reduction techniques used at Langley to determine heat transfer characteristics from phosphor data.

### Step Injection Method

The step injection method for determining heat transfer coefficients is basically the same as the procedure used in the reduction of phase-change paint data outlined in reference 7 with a couple of modifications. With this procedure, the injection process is modelled as a step with the heat transfer coefficient at each point of the model undergoing a sudden jump and then remaining constant throughout the run. Mathematically this is shown by applying the following convective condition

$$\dot{q}_s = -h[\theta_{aw} - \theta(0, t)] \quad (9)$$

Substituting the transform of equation (9) into equation (8) and taking the inverse transform of the combination results in the following equation for the step injection method:

$$\frac{\theta_{ph}}{\theta_{aw}} = 1 - e^{\lambda^2} \operatorname{erfc} \lambda \quad (10)$$

where

$$\lambda = \frac{h\sqrt{t}}{\beta} \quad (11)$$

The step time,  $t$ , in equation (11) can be determined from thin-film time histories through the injection process. By modelling the rise in heat transfer coefficient as a model makes its way through the tunnel boundary layer as a ramp-step, an effective step time can be determined. While such a step time is dependent on the model geometry, model angle of attack, and the pressure differential between the tunnel and the sheltered injection chamber, it can be assumed to be constant at every point

on the model if the injection of the model into the flow is rapid. For the 31-Inch Mach 10 Tunnel, this step time has been calculated to be approximately 1 second with an error of 3.0 percent. For a given injection system, this number should remain fairly constant from run to run.

Another method of determining the effective step time has been attempted but has met with very little success. Since this data reduction method makes the assumption that the heat transfer coefficient is constant at all times, the following assumption at a location on the model might be made:

$$h_1 = h_2 = \frac{\lambda_1}{\sqrt{t_1}} = \frac{\lambda_2}{\sqrt{t_2}} \quad (12)$$

The first step time might then be found from Equation (14) as

$$t_1 = \frac{\lambda^2 \Delta t_{12}}{\lambda_2^2 - \lambda_1^2} \quad (13)$$

Unfortunately, equation (13) is very sensitive to conduction on a model, any change in the adiabatic wall temperature, or any noise in the data. No meaningful effective step time can be determined if these effects are large.

A menu-driven program, called PHOS4 has been developed to reduce phosphor thermography data using the step injection technique quickly and efficiently. Because of the fact that  $T_{aw}$  is variable and because there is a slight spacial scatter in the initial time images, the program solves equation (10) for all of the 262 thousand points on a phosphor image. In order to handle the large number of points, a closed form solution procedure has been derived for equation (10) which solves for the heat transfer coefficient at a point. PHOS4 runs on a 386-based Compac computer and computation time for each run is approximately four minutes. Heat transfer results are stored in a binary image file which can be viewed on the video acquisition system or on any computer which uses a standard image processing package. Results can also be printed out via a color printer.

A comparison has been made between thermographic phosphor data and thin-film data on the windward side of an orbiter-like configuration<sup>8</sup>. Phosphor data were compared to measurements with thin-film gages (which have an accuracy of 5 to 8 percent) mounted on the windward side of the model along the centerline and spanwise gages at 65, 75 and 85 percent of the model length as shown in Figure 4. Runs were made using the thin-film model and the ceramic phosphor model at an angle of attack of 20° and a Reynolds number

of  $0.5 \times 10^6$ /foot in the 31-Inch Mach 10 Tunnel; both models were 10 inches long. Heat transfer results were calculated using the PHOS4 data reduction program and nondimensionalized by the stagnation point heat transfer of a 0.2067 inch sphere (Fig. 5). The majority of the scatter seen in the phosphor data is caused by the rough phosphor coating on the model surface as noted in the model fabrication discussion. Overall, the phosphor data appear to compare favorably with the thin-film data. Indeed, in regions where there are local maxima, such as the shock interaction regions seen at  $x/L=.75$  and  $.85$  (Figs. 5(c) and 5(d)), the phosphors provide a better indication than the thin-film gages for the absolute magnitude of heating occurring on a model unless the thin-film gages are placed close enough together to completely capture the presence of such heating spikes. There are some cases where the two acquisition methods disagree somewhat, such as in the over-prediction of the heating at  $x/L=.85$  (Fig. 5(d)) or in the nose region on the centerline plot (Fig. 5(a)). One possible cause for some of this disparity in the data may be due to the fact that the present phosphor system can not yet accurately locate each image pixel on the model. Thus, in regions where there are higher heat transfer coefficient gradients, a small deviation from an assumed location can result in a large amount of error in the calculated heat transfer coefficient for that location. This problem could be corrected in a couple of ways. Reference points or lines might be drawn on a model or target recognition software could be used as will be considered in conjunction with a new phosphor system to be discussed later in this paper.



### Curve-Fit Method

Another method for reducing phosphor thermography data has been developed by G.M. Buck<sup>3</sup>. This procedure uses the following convective boundary condition

$$\dot{q}_s(t) = A(B - \theta_s(t)) \quad (14)$$

where A and B are variable coefficients. Substituting the Laplace transform of equation (14) back into equation (8) and taking the inverse transform of the result yields

$$\theta_s(t) = B(1 - e^{(\frac{A}{\beta})^2 t} \operatorname{erfc}(\frac{A}{\beta} t^{\frac{1}{2}})) \quad (15)$$

Equation (15) is similar to the governing step injection equation (equation (10)) and indeed it is the same if  $A=h$  and  $B=T_{aw}$ . The major difference between the two equations is that  $T_{aw}$  does not explicitly show up in equation (15); thus  $T_{aw}$  does not need to be known in order to carry out the computations.

In order to use equation (15) a temperature-time history is required for each point after the model has been completely injected. Assuming that the heat conduction is normal into the model, equation (15) can then be fit to the temperature history and the resulting A and B coefficients are substituted back into equation 16 to obtain heat transfer values. In order to obtain heat transfer coefficients at a point, the resulting heat transfer values can be substituted back into the definition of the convective heat transfer:

$$h = \frac{\dot{q}}{T_{aw} - T_s} \quad (16)$$

This curve-fit method has provided values of the heat transfer rate that are in fairly good agreement with thin-film results.<sup>3</sup> By taking out the adiabatic wall temperature, one source of error is eliminated during the data reduction. One drawback to the technique, however, is that the heat conduction must be one dimensional in nature or else the curve fitting procedure will not work. Also, data must be acquired at a point a substantial amount of time after the model has reached the nozzle centerline to obtain an accurate curve-fit. Unfortunately in some situations this

cannot be afforded because conduction effects may become significant or the phosphors themselves may get hot enough to quench.

### Thin-Film Method

Heat conduction within the model can be significant especially in the nose region of models and on control surfaces. To uphold a 1-D assumption, heat transfer coefficients must be obtained early into the run. Unfortunately, use of the previously described reduction procedures with shorter run times yields inaccurate results because in the case of the step injection technique, the initial temperature rise is significant and in the curve-fitting technique, there are not enough data points to make an accurate curve fit. In this case the complete heating history at each point on the model surface of interest must be used to obtain accurate results.

A few techniques have been considered which would integrate temperature-time histories into the data reduction. The triangular pulse method developed by P.R. Hill<sup>9</sup> is presently being examined but conclusions on its applicability to phosphors and its accuracy still have not been made. Another possibility is to carry out a numerical analysis by using finite differences on Equation (4). A time dependent scheme could be used with the phosphor data as a known boundary condition. This technique however requires a relatively large amount of computational time as well as memory. Presently, the most promising time series technique for application to thermographic phosphor data appears to be the equation used to reduce thin-film data. With a high enough acquisition frequency, this equation is reasonably accurate<sup>10</sup> and its application to phosphor images is fairly straight forward.

The thin-film equation can be found by first putting equation (8) in terms of the transformed heat transfer and then taking the inverse of the equation to obtain:

$$\dot{q}_s = \sqrt{\frac{\rho c k}{\pi}} \int_0^t \frac{dT(\tau)}{(t-\tau)^{1/2}} d\tau \quad (17)$$

Equation (17) can be integrated by parts to yield:

$$\dot{q}_s = \sqrt{\frac{\rho c k}{\pi}} \left[ \frac{T(t)}{\sqrt{t}} + \int_0^t \frac{T(t) - T(\tau)}{(t-\tau)^{3/2}} d\tau \right] \quad (18)$$

Unfortunately, a singularity arises in the integrand in equation (18) when  $\tau$  approaches  $t$ . In order to circumvent this problem,

Cook<sup>11,12</sup> derived the following equation

$$\dot{q}_s = 2\sqrt{\frac{\rho c k}{\pi}} \sum_{i=1}^n \frac{T(t_i) - T(t_{i-1})}{\sqrt{t_n - t_i} + \sqrt{t_n - t_{i-1}}} \quad (19)$$

Equation (19) assumes that the thermal properties are constant throughout the run. By using the time history of a given point on a model throughout a run with equation (19), the heat transfer at a point can be determined for any time during the run. The heat transfer coefficient,  $h$ , can then be determined by using the definition for convective heat transfer (equation 16).

One of the problems with attempting to use a thin-film type analysis with the thermographic phosphor system is that images must be obtained throughout model injection. To do this however, the camera has to be focused on the model throughout the injection, which is not a trivial task. One way to solve this problem would be to mount the camera and ultraviolet lights on the back side of the injection plate with windows installed on the plate so that the camera could focus on the model and the UV lights could illuminate the model. Such a setup would be difficult to install since it would have to compete with the host of other types of instrumentation typically mounted to the back of the plate. In addition, there would be the question of whether or not the camera and lens could endure the loads associated with the injection process. Another possibility for obtaining constant focus during injection would be to station the camera on the side of the tunnel looking through an optical window and have the lens automatically zoom out. Since the model injection process is usually less than a second, getting the lens to accurately zoom on the model may be impractical.

In order to stay in focus through the injection process, the depth of field of a camera lens was used. The depth of field is basically a range of distances over which an object is visually in focus. By increasing the lens factor setting on a lens (closing the aperture), the depth of field can be increased. Thus if there is enough light, if a camera is set up correctly, and if the tunnel being used is not extremely large, a depth of field can be obtained which is large enough such that a model is completely in focus during the injection process. To set up a camera in such a way that a wind tunnel model is in focus throughout the injection process, the model is positioned in the wind tunnel at the optimum focusing location and the camera is focused on the model as sharply as possible. The optimum focusing position can be determined from optical equations as

$$e_o = 2d_o \left[ \frac{f_o}{d_o + f_o} \right] \quad (20)$$

As shown in Fig. 6,  $d_o$  is the distance between the lens plane and the farthest point away that the model has to be in focus (i.e. the tunnel wall);  $f_o$  is the distance between the lens plane and the closest point that the model has to be in focus (i.e. the injection limit) and  $e_o$  is the distance between the lens plane and the point for optimum focusing.

In order to determine whether using thin-film equations with the thermographic phosphors was practical, a calibration hemisphere was fabricated and tested. The hemisphere was tested in the 31-Inch Mach 10 Tunnel at a freestream unit Reynolds number of  $0.5 \times 10^6/\text{foot}$ . One run was made with a runtime of just over one second. The camera framing rate was 30 frames per second. One issue which was of concern was whether or not the hemisphere would receive enough UV illumination, but no illumination problem was experienced during the run. The UV lights were focused on the centerline where the model would be the hottest and thus in the most danger of having the phosphors quench. A review of the acquired images after the test revealed that the phosphors on the model did not quench at any time during the run and that the model remained in focus throughout the injection process.

Data reduction was carried out for just the centerline of the images. A fourth order Chebyshev polynomial fit was applied spatially for each time to reduce the scatter of the phosphor data. Heat transfer was calculated using Equation (19) and then heat transfer coefficients were calculated using Equation (16). The heat transfer coefficients were then nondimensionalized by the maximum heating on the hemisphere and the results were compared with predictions of a Lees distribution<sup>13</sup> and a time-dependent boundary layer code (Fig.7). Measured heating on the hemisphere is higher than Lees theory or computations predict -- at least for sphere angles less than  $70^\circ$ . Towards the shoulder of the hemisphere the boundary layer code predicts higher heating than the Lees distribution. The experimental heat transfer meanwhile drops down coincidentally to the values predicted by the Lees distribution. One possible explanation for the differences in trends may again (as with the orbiter comparison) be that the exact location of each point on the model is not accurately known. In addition, due to the limited memory capability of the present system, the data shown in the plot corresponded to 0.8 second after the model had first been exposed to the tunnel flow (i.e. started into the tunnel boundary layer). At  $t=0.8$  second the model was still moving and had not reached the centerline. Thin-film data from other experiments carried out in the 31-Inch Mach 10 Tunnel show that the heat transfer rises slightly through injection. To be confident that the data are not seeing this rise in heat transfer rate, one second from the time the model is first exposed to the tunnel flow must usually be allowed for. Time traces from the hemisphere in this case showed that near the front of the model the heat transfer had begun to fall at 0.8 second but farther back it was still rising. Thus one might expect the heat transfer distribution to

exhibit some nonideal characteristics. Even so, the phosphor and thin-film data are qualitatively similar and the technique shows promise.

### Next-Generation System

In order to solve some of the problems mentioned with the present thermographic phosphor technique and to acquire new capabilities, a new phosphor system is being purchased and delivery is expected before the end of 1991. One of the issues to be addressed is the problem of knowing precisely where an image pixel point is located on a wind tunnel model. In addition, when the depth of field method is utilized with the camera, the image incidence angle actually changes through injection. In order to overcome these difficulties, target recognition software is being used to track the model throughout a wind tunnel test. To use this software, the model geometry is entered into the acquisition computer and during a run, sixteen points are simultaneously tracked. The software handles any spatial transformations and it treats image interpolations using a frequency mapping.

For increased accuracy in heat transfer data reduced using the thin-film equations, the new system will acquire phosphor images at a minimum of 30 frames per second. In order to store the vast amounts of data which will be created, test results will be saved on a studio video recorder. Data for a given run can be read off the recorder and digitized at real-time rates.

Another problem with the present phosphor system which has not previously been discussed is that each camera pixel is assumed to produce the same response for a given intensity of light. There is, however, some variation between pixels and this results in data scatter which is in addition to the scatter caused by the rough phosphor surface. In order to handle this, the new system will include a calibration procedure which includes the response of each individual camera pixel.

One difficulty with the two-color phosphor technique is that the temperature range obtainable with just two phosphors is limited. To increase this range, three phosphors could possibly be used. The new phosphor system will be able to accommodate three phosphors if required.

Another problem which is sometimes experienced when aerothermodynamic data are acquired, particularly on a slender body or a control surface, is the presence of conduction effects. In order to study this in more detail, the new injection plate mirror on the 31-Inch Mach 10 Tunnel could be used to gain a second view of the model. Using two synchronized CCD cameras, the new system will be able to obtain the temperature distribution for just about every point on a wind tunnel model. Integrating these results with a computational code will allow the study of 3D conduction effects.

### Concluding Remarks

The relative-intensity two-color phosphor thermography system has become an integral part of aerothermodynamic measurement techniques used in the Langley Hypersonic Facilities Complex. The present system has matured to a point where it is more than just a system for qualitative studies. It can provide quantitative heat transfer distributions about a model with an accuracy comparable to that of thin-film gages. In addition, fabrication techniques for phosphor models are constantly being developed and improved and the ceramic investment casting technique represents a significant advancement in this area. Also, the addition of phosphors directly to the model material shows some potential for decreasing the scatter seen in phosphor thermography images. To date, the phosphor system has been used primarily in the 31-Inch Mach 10 Tunnel; however the system is scheduled for use in the 15-Inch Mach 6, the 20-Inch Mach 6  $CF_4$ , the 20-Inch Mach 17 Nitrogen, and the 22-Inch Mach 20 Helium Tunnels in the near future. One approach which shows some promise in increasing the accuracy in heat transfer data is the application of the thin-film equations. This technique includes the time history of the heating on a model and thus if refined properly has the potential for being more accurate than the step-injection method. In addition, it has an advantage over both the step-injection method and the curve-fit method in that the run times can be substantially shorter, thus reducing the departure from one-dimensional behavior via conduction effects.

To obtain data using the thin-film technique, a new system is being assembled. This system will represent a significant step forward for the phosphor technique at Langley with one of its primary attributes being the addition of target recognition type software to help in quantitatively determining the location of each pixel on a model phosphor image. Other features of this system will include individual camera pixel calibration, increased data handling efficiency and the ability to process three colors for three-color phosphor thermography.

### Acknowledgements

The author acknowledges the contributions of the following people: G. M. Buck of Langley's Experimental Hypersonics Branch (EHB) who gave mentorship on the phosphor technique, J. R. Micol of the EHB who provided the thin-film data for comparison with the phosphor results, Pete Vasquez, of Langley's Composite Models Development Section for his in-depth explanation of the investment casting procedure, H. H. Hamilton of Langley's Aerothermodynamic Branch who computed the predictions for heating about the sphere, and H. David Kaysen of M. Rosenblatt and Son for his suggestion of using the lens depth of field for obtaining time series data with the thermographic phosphor system.

## References

- <sup>1</sup>Buck, G.M., "An Imaging System for Quantitative Surface Temperature Mapping Using Two-Color Thermographic Phosphors," Paper presented at the 34th International Instrumentation Symposium, May 2-5, 1988.
- <sup>2</sup>Buck, G.M., "Automated Thermal Mapping Techniques Using Chromatic Image Analysis," NASA TM-101554, April 1989.
- <sup>3</sup>Buck, G.M., "Surface Temperature / Heat Transfer Measurement Using a Quantitative Phosphor Thermography System," AIAA Paper 91-0064.
- <sup>4</sup>Miller, C.G., "Langley Hypersonic Aerodynamic/Aerothermodynamic Testing Capabilities -- Present and Future," AIAA Paper No. 90-1376, 1990.
- <sup>5</sup>Schultz, D.L. and Jones, T.V., "Heat-Transfer Measurements in Short-Duration Hypersonic Facilities," AGARD AG-165, 1973.
- <sup>6</sup>Buck, G.M. and Vasquez, P., "An Investment Ceramic Slip-Casting Technique for Net-Form, Precision, Detailed Casting of Ceramic Models," NASA Disclosure No. LAR 14471-1, April 1990.
- <sup>7</sup>Jones, R.A. and Hunt, J. L., "Use of Fusible Temperature Indicator for Obtaining Quantitative Aerodynamic Heat Transfer Data," NASA TR R-230, Feb. 1966.
- <sup>8</sup>Micol, J.R., "Aerothermodynamic Measurement and Prediction for a Modified Orbiter at Mach 6 and 10 in Air," AIAA Paper 91-1436.
- <sup>9</sup>Hill, P.R., "A Method of Computing the Transient Temperature of Thick Walls From Arbitrary Variation of Adiabatic-Wall Temperature and Heat-Transfer Coefficients" NACA Report 1372, 1958.
- <sup>10</sup>Miller, C.G., "Comparison of Thin-Film Resistance Heat-Transfer Gages With Thin-Skin Transient Calorimeter Gages in Conventional Hypersonic Wind Tunnels," NASA TM 83197, 1981.
- <sup>11</sup>Cook, W.J. and Felderman, E.J., "Reduction of Data from Thin-Film Heat-Transfer Gages: A Concise Numerical Technique," AIAA Journal, March 1966.
- <sup>12</sup>Cook, W.J., "Determination of Heat-Transfer Rates from Transient Surface Temperature Measurements," AIAA Journal, July 1970.
- <sup>13</sup>Lees, Lester, "Laminar Heat Transfer Over Blunt-Nosed Bodies at Hypersonic Flight Speeds," Jet Propulsion, Vol. 26, No.4, April 1956.

Table 1. The Langley Hypersonic Facilities Complex

20-Inch Mach 6 CF <sub>4</sub> Tunnel
20-Inch Mach 6 Tunnel
15-Inch Mach 6 Hi Temperature Tunnel
12-Inch Mach 6 Hi Pressure Tunnel
18-Inch Mach 8 Tunnel
31-Inch Mach 10 Tunnel
20-Inch Mach 17 Nitrogen Tunnel
60-Inch Mach 18 Helium Tunnel
22-Inch Mach 20 Helium Tunnel



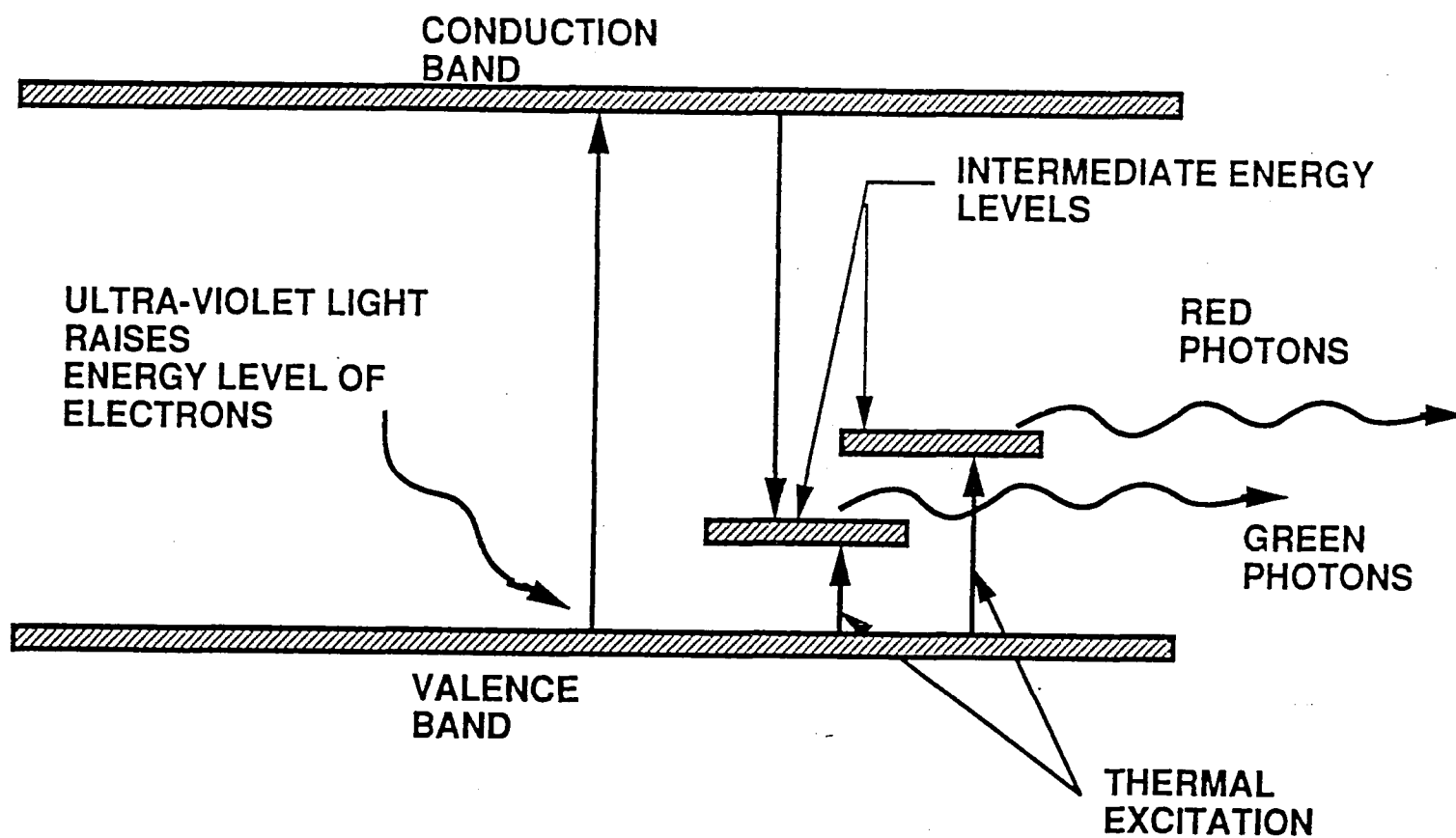


Figure 1. Energy level diagram for a two-color phosphor.

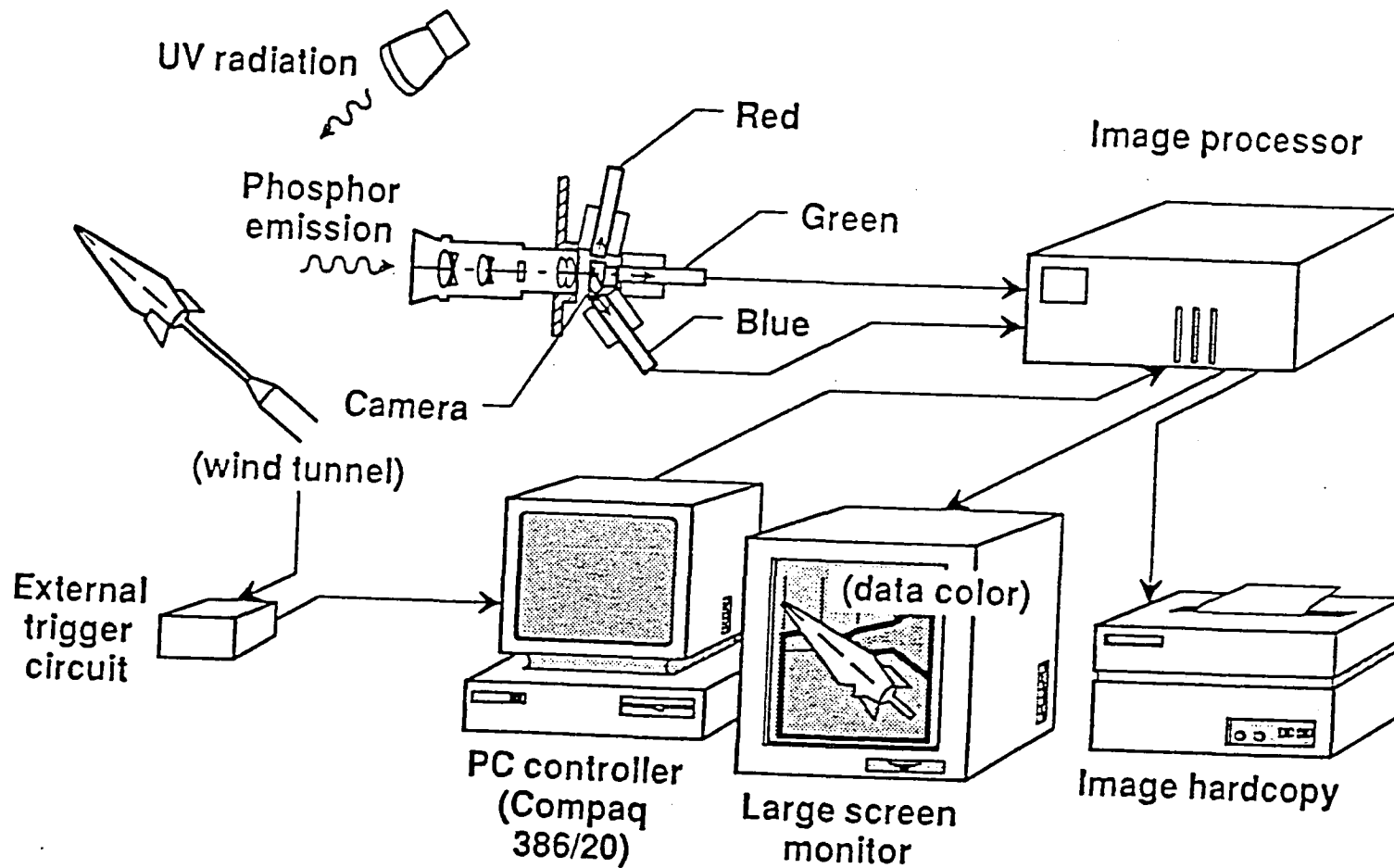


Figure 2. The relative-intensity phosphor thermography system.

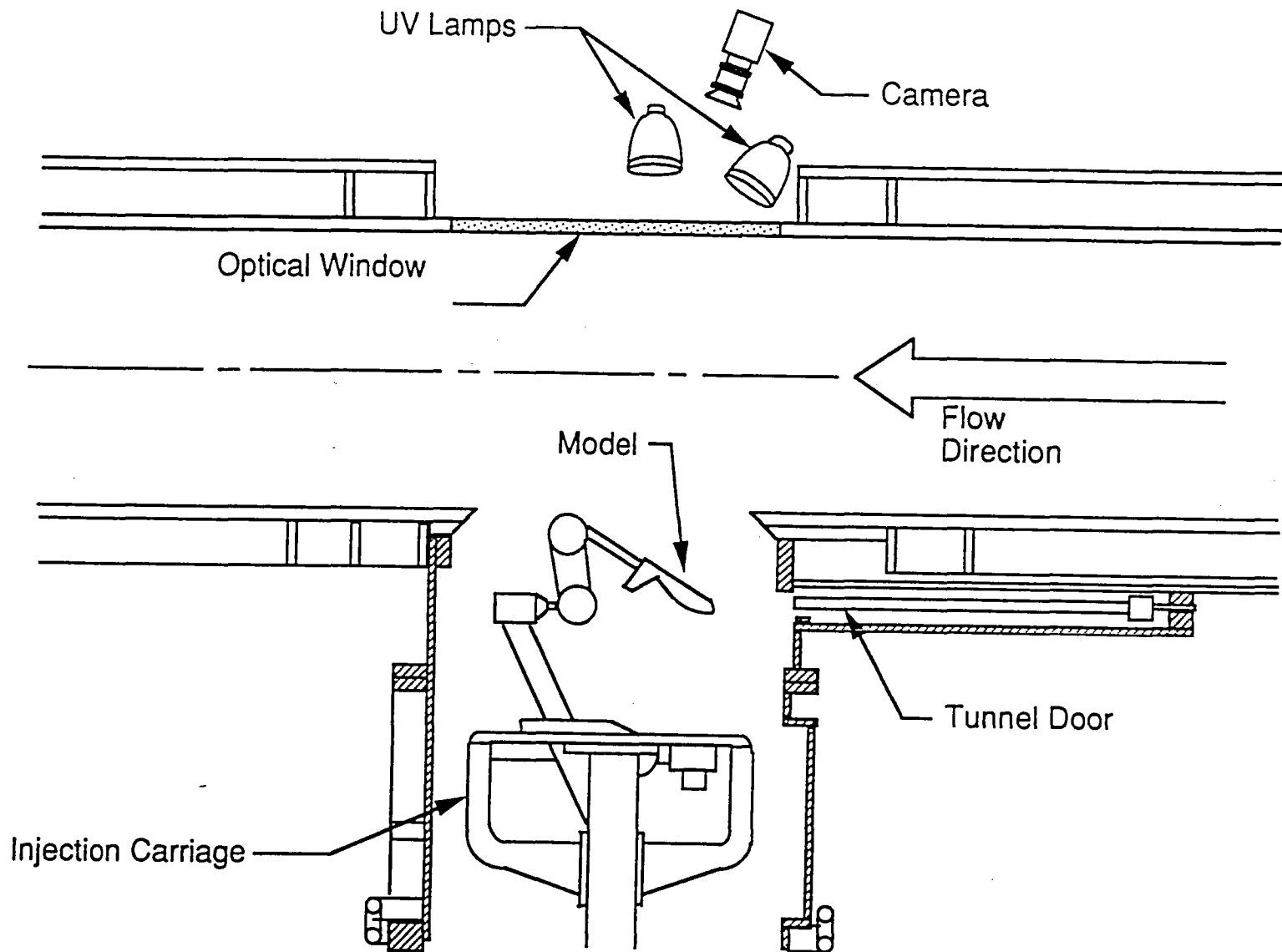


Figure 3. 31-Inch Mach 10 Tunnel test section.

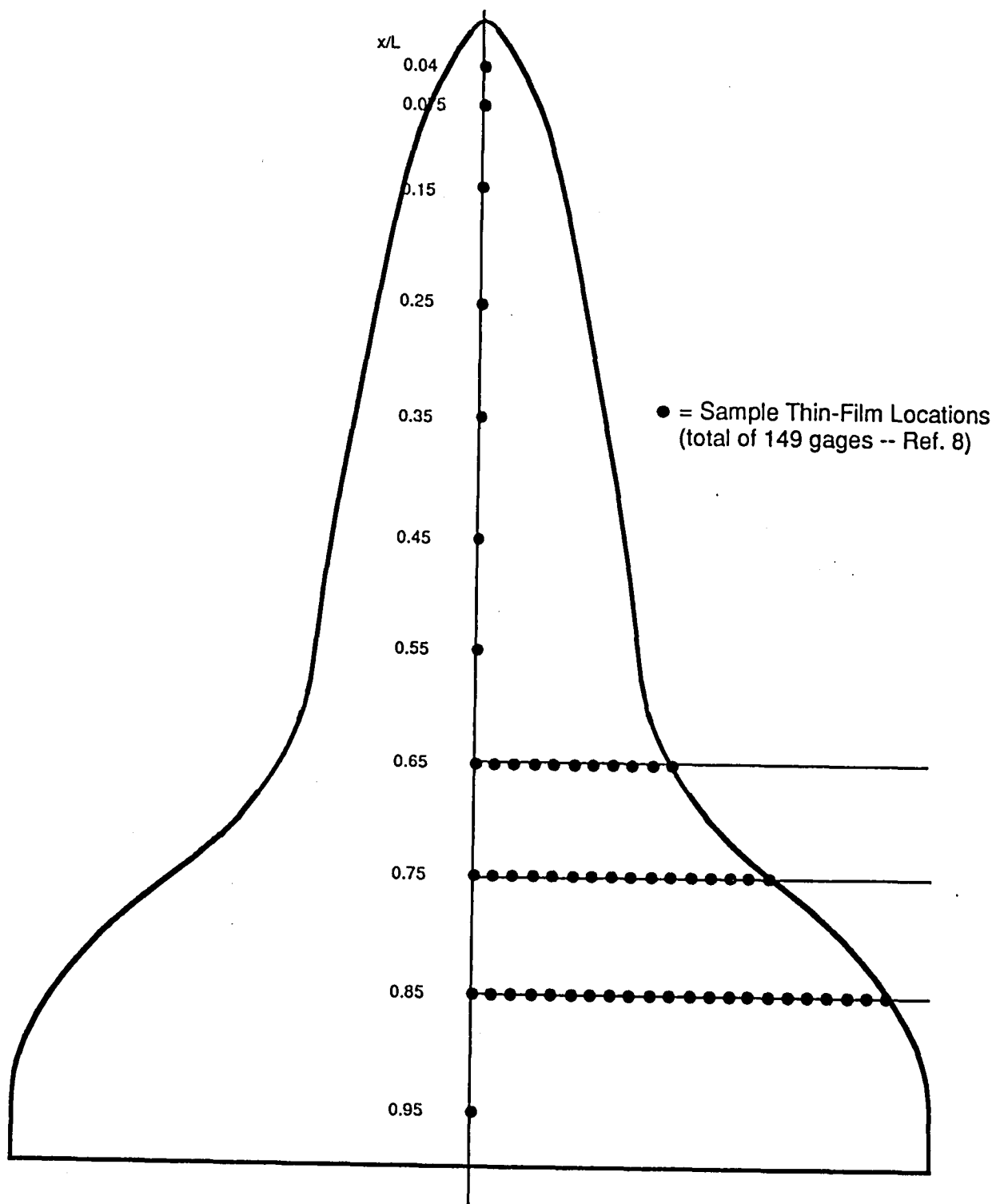
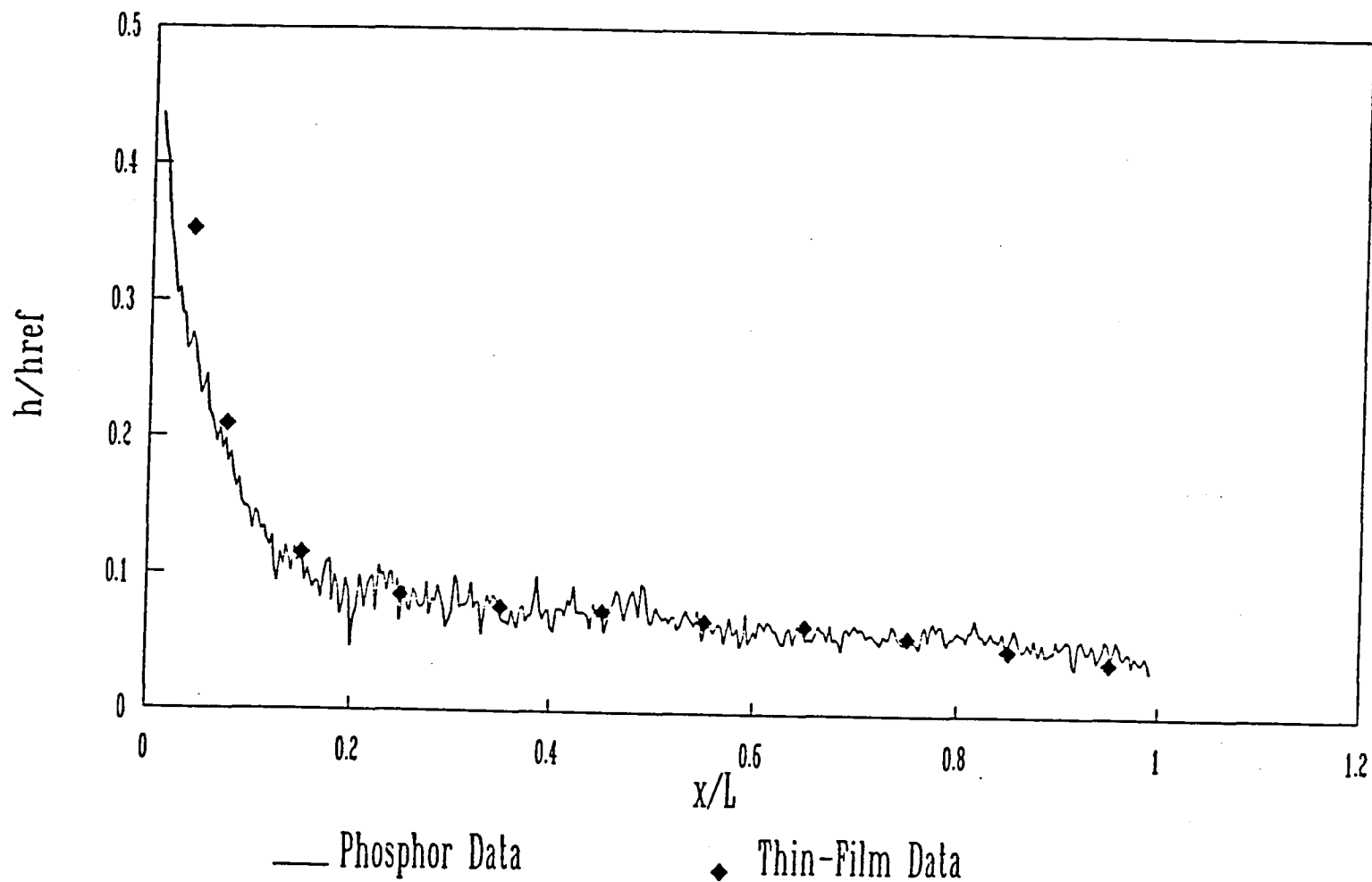
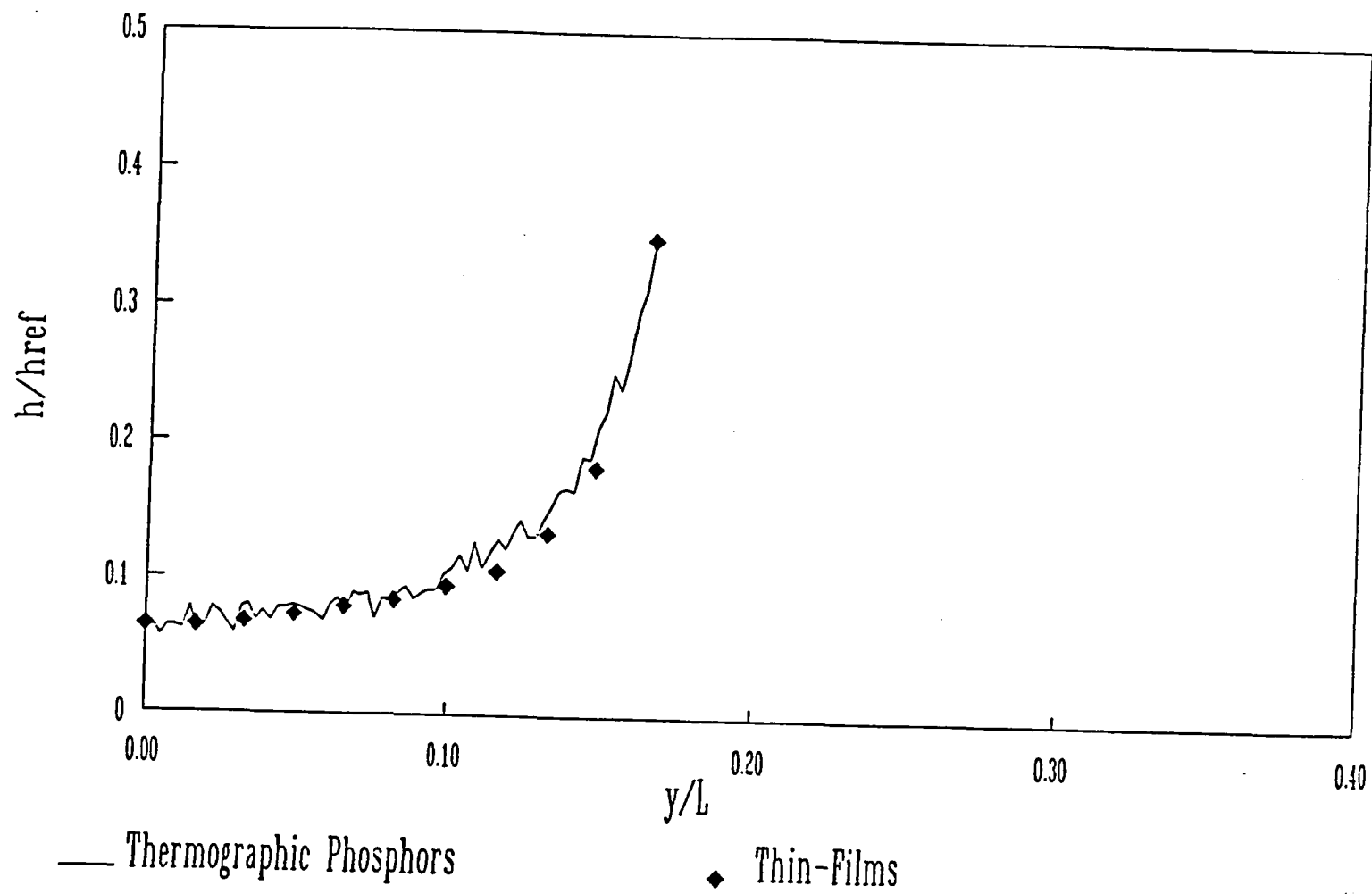


Figure 4. Locations of phosphor and thin-film measurements on windward surface of modified orbiter-like configuration.



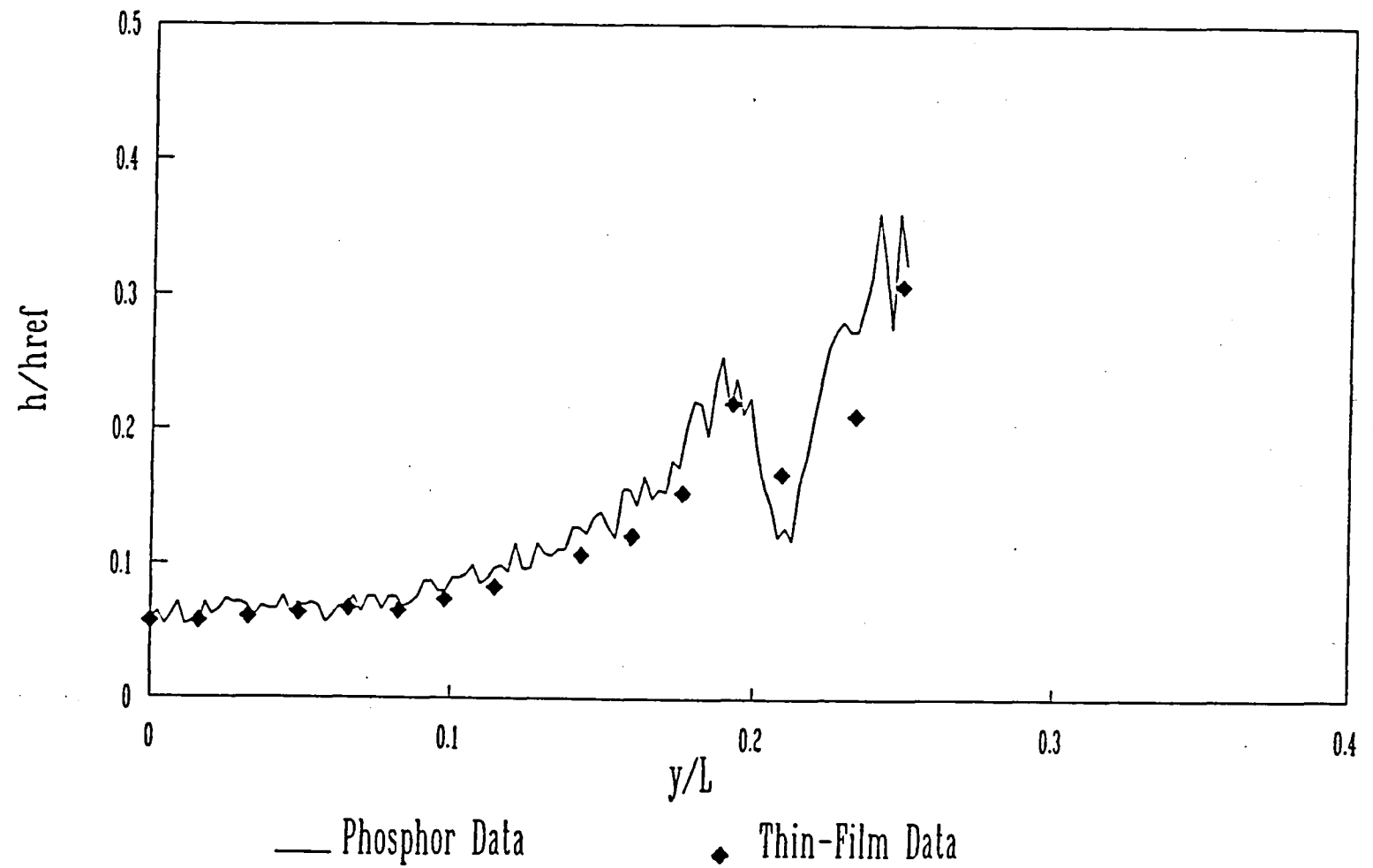
(a) Centerline

Figure 5. Comparison of thin-film and phosphor data on an orbiter-like configuration.  
Mach # = 10,  $Re = 500,000$  /ft., AOA = 20 deg.

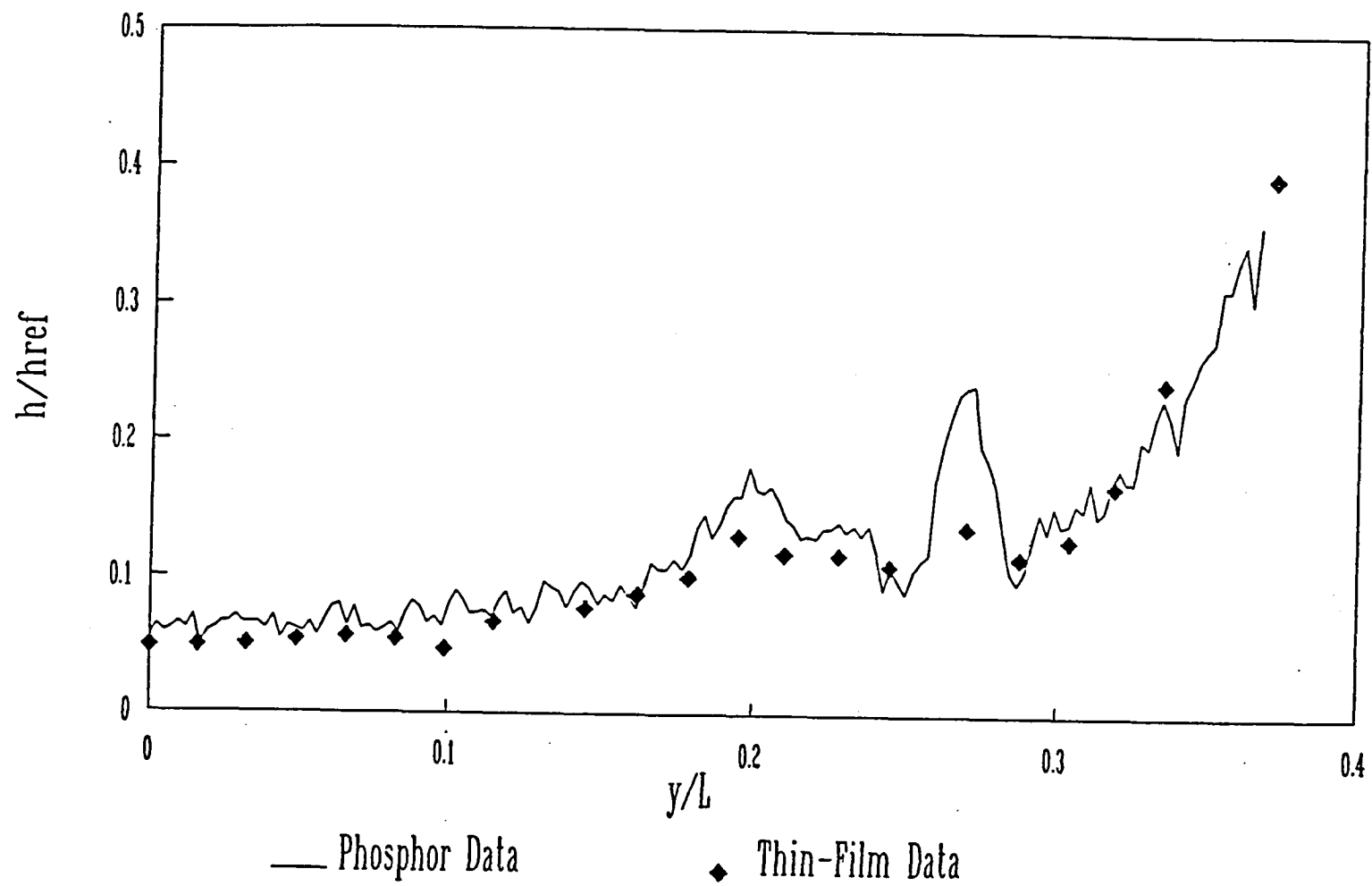


(b)  $x/L=0.65$

Figure 5. - Continued



(c)  $x/L=.75$   
Figure 5. - Continued



(d)  $x/L = 0.85$

Figure 5. - Continued



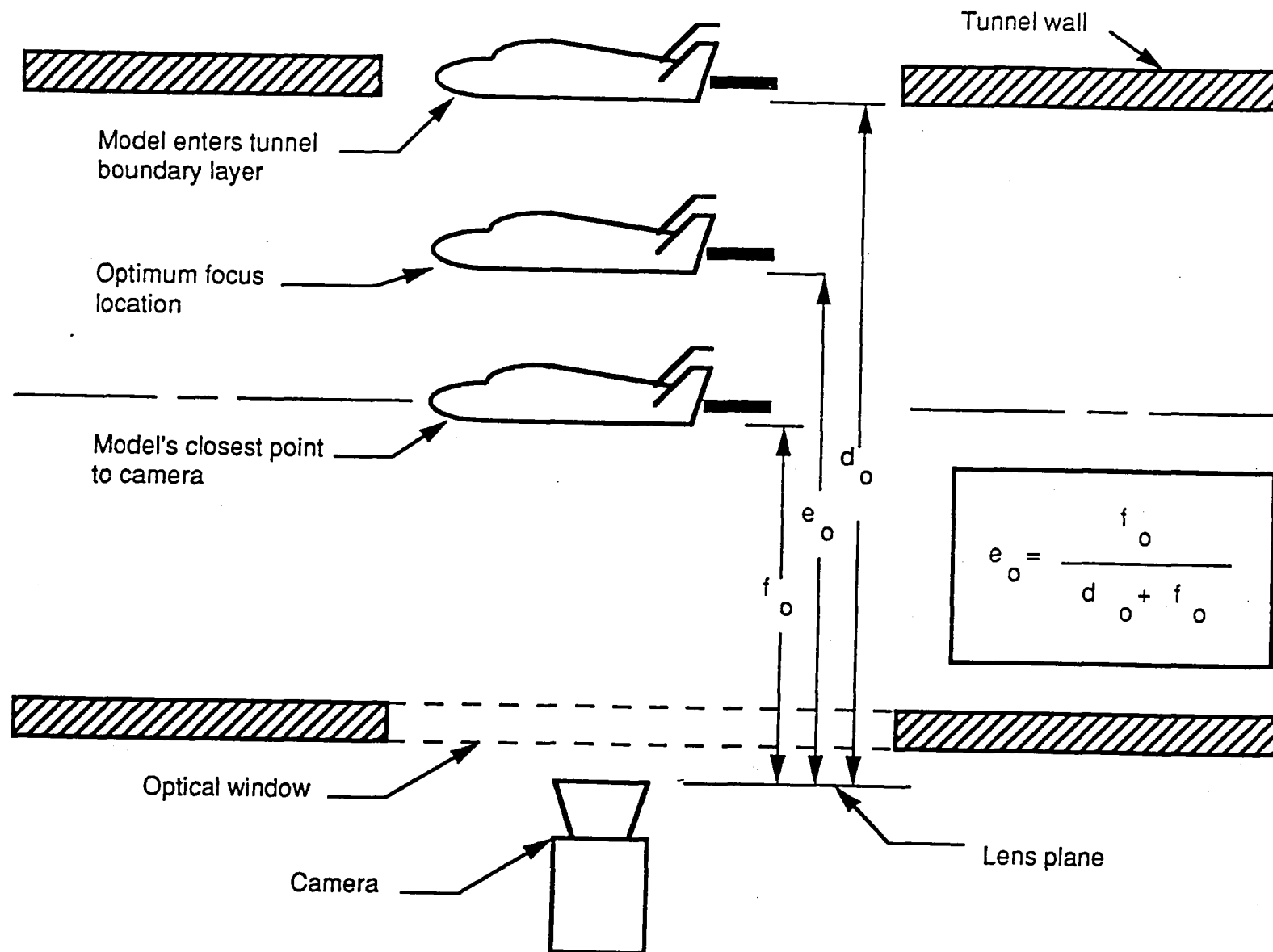


Figure 6. Determination of optimum focus point.

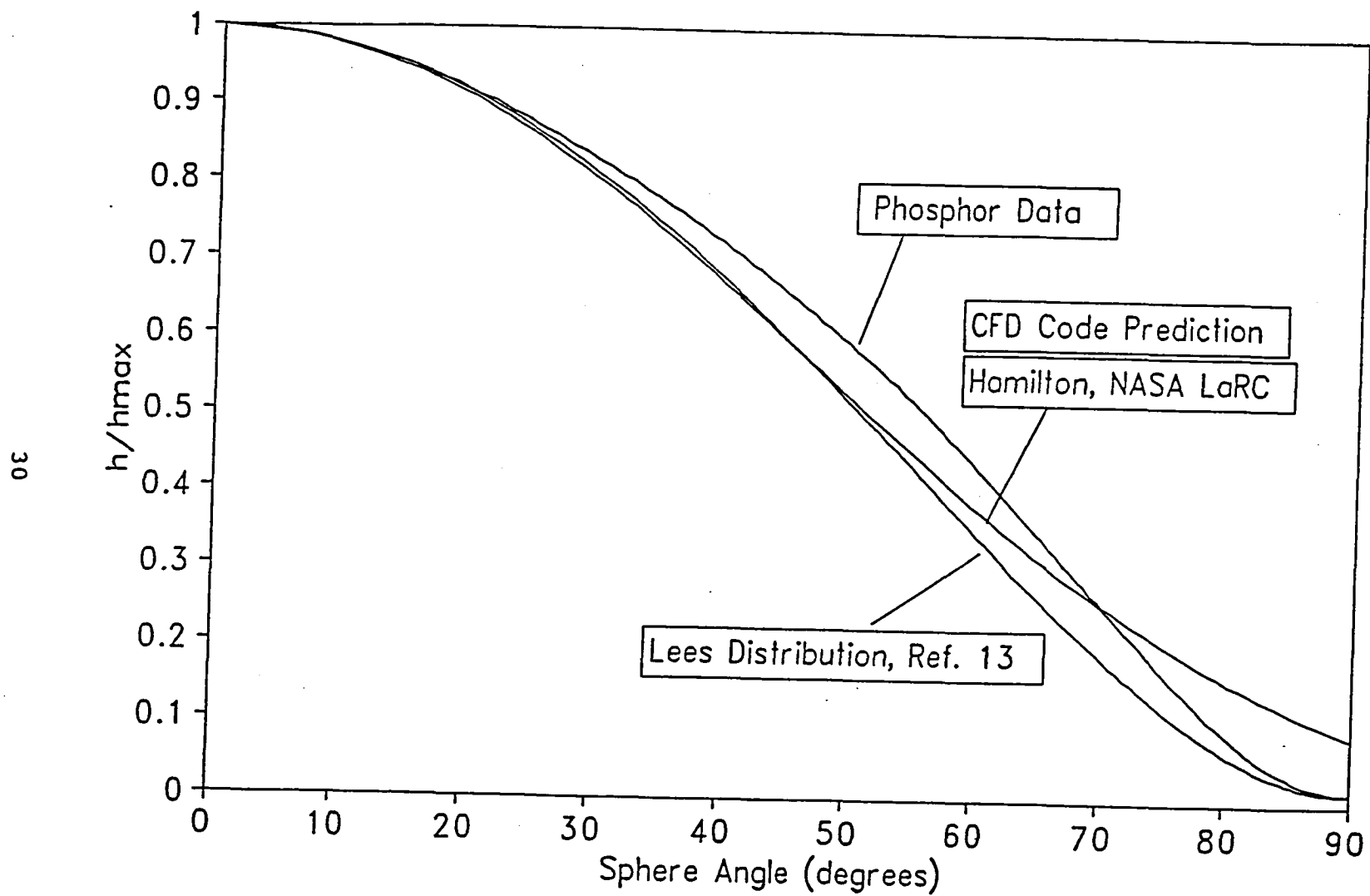


Figure 7. Heat transfer about a sphere.  
Mach #=10, Re=500,000 /ft.





## Report Documentation Page

1. Report No. NASA TM-104123		2. Government Accession No.		3. Recipient's Catalog No.	
4. Title and Subtitle  A Relative-Intensity Two-Color Phosphor Thermography System				5. Report Date  September 1991	
				6. Performing Organization Code	
7. Author(s)  N. Ronald Merski				8. Performing Organization Report No.	
				10. Work Unit No.  506-40-41-02	
9. Performing Organization Name and Address  NASA Langley Research Center Hampton, VA 23665-5221				11. Contract or Grant No.	
				13. Type of Report and Period Covered  Technical Memorandum	
12. Sponsoring Agency Name and Address  National Aeronautics and Space Administration Washington, DC 20546-0001				14. Sponsoring Agency Code	
15. Supplementary Notes					
16. Abstract  The NASA Langley Research Center has developed a relative-intensity two-color phosphor thermography system. This system has become a standard technique for acquiring aerothermodynamic data in Langley's Hypersonic Facilities Complex (HFC). The relative intensity theory and its application to the Langley phosphor thermography system is discussed along with the investment casting technique which is critical to the utilization of the phosphor method for aerothermodynamic studies. Various approaches to obtaining quantitative heat transfer data using thermographic phosphors are addressed and comparisons between thin-film data and thermographic phosphor data on an orbiter-like configuration are presented. In general, data from these two techniques are in good agreement. A discussion is given on the application of phosphors to integration heat transfer data reduction techniques (i.e., the thin-film method) and preliminary heat transfer data obtained on a calibration sphere using thin-film equations are presented. Finally, plans for a new phosphor system which uses target recognition software are discussed.					
17. Key Words (Suggested by Author(s))  Phosphor Thermography Phosphors			18. Distribution Statement  Unclassified-Unlimited Subject Category - 34		
19. Security Classif. (of this report)  Unclassified		20. Security Classif. (of this page)  Unclassified		21. No. of pages  32	
				22. Price  A03	



